

Approved for public release;
distribution is unlimited.

Title: Real-Time Alphas Emitter Assay
of Large Volumes

Author(s): Phillip L. Kerr, NIS-6
James E. Koster, NIS-6
Kevin Macy, NIS-6
Jay Cook, NIS-6

RECEIVED
DEC 26 1996
OSTI

Submitted to: Waste Management '97
March 2-7, 1997
Tucson, AZ

Decontamination and Decommissioning

DISCLAIMER

This report was prepared as an account of work sponsored by an agency of the United States Government. Neither the United States Government nor any agency thereof, nor any of their employees, makes any warranty, express or implied, or assumes any legal liability or responsibility for the accuracy, completeness, or usefulness of any information, apparatus, product, or process disclosed, or represents that its use would not infringe privately owned rights. Reference herein to any specific commercial product, process, or service by trade name, trademark, manufacturer, or otherwise does not necessarily constitute or imply its endorsement, recommendation, or favoring by the United States Government or any agency thereof. The views and opinions of authors expressed herein do not necessarily state or reflect those of the United States Government or any agency thereof.

MASTER

Los Alamos
NATIONAL LABORATORY

DISTRIBUTION OF THIS DOCUMENT IS UNLIMITED

Los Alamos National Laboratory, an affirmative action/equal opportunity employer, is operated by the University of California for the U.S. Department of Energy under contract W-7405-ENG-36. By acceptance of this article, the publisher recognizes that the U.S. Government retains a nonexclusive, royalty-free license to publish or reproduce the published form of this contribution, or to allow others to do so, for U.S. Government purposes. Los Alamos National Laboratory requests that the publisher identify this article as work performed under the auspices of the U.S. Department of Energy. The Los Alamos National Laboratory strongly supports academic freedom and a researcher's right to publish; as an institution, however, the Laboratory does not endorse the viewpoint of a publication or guarantee its technical correctness.

DISCLAIMER

**Portions of this document may be illegible
in electronic image products. Images are
produced from the best available original
document.**

REAL-TIME ALPHA EMITTER ASSAY OF LARGE VOLUMES

P. L. Kerr
J. E. Koster
Kevin Macy
Jay Cook

Los Alamos National Laboratory
Los Alamos, NM 87545

Paper to be submitted to Waste Management '97, March 2-7, 1997, Tucson, AZ
Topic: 5.3. Decontamination and Decommissioning

ABSTRACT

Detection of contamination within large volumes or pipes is important for the processes of decontamination and decommissioning and for the transportation and disposal of hazardous waste. Alpha emitter contamination has been particularly difficult to assay because of the short range of alpha particles in air — about 5 cm. In addition, real-time sensitive monitoring of long or small enclosures, or of large volumes with complicated internal geometries, is very difficult or impossible with traditional alpha detectors.

However, the ionization detection method (long-range alpha detection, or LRAD) in development at Los Alamos National Laboratory detects the air molecules ionized by alpha particles (rather than the alpha particles themselves), and these ions can travel long distances through enclosed volumes (several meters). In addition, a single 5-MeV alpha particle produces approximately 140,000 ions, and so even an incomplete collection of the ions will produce a significant signal as opposed to a traditional alpha detector which either detects or fails to detect a single alpha even. The LRAD method therefore offers significant advantages over other detector schemes.

The LRAD detector works by collecting of ionized air molecules on a grid or on parallel plates held at 100-300 V. Ions move into the detector either by thermal motion or by a fan, and the current produced is measured by a very sensitive electrometer. For larger volumes, higher airflows and detector voltages are required to maintain the same sensitivity to alpha contamination. In addition, the parallel plates are the preferred method for high airflows because of reduced turbulence.

We will present the results of tests of a High Airflow Monitor alpha detector and draw conclusions about the optimum configuration for specific assay applications. Detector parameters examined include varying voltages, grid and plate geometries, airflow rates, and whether the signal originates from the neutral plates or the plates at high voltage.

INTRODUCTION

In this paper we discuss the design and behavior of a High Airflow Monitor (HAFM) based on Long-Range Alpha Detector (LRAD) technology [1]. The low air resistance construction of the HAFM enables the high airflow crucial for assay of rooms, vaults, or cargo vehicles. This is accomplished by orienting plates parallel to the airflow rather than perpendicular, as are the grids in other LRADs.

As will be shown in this paper, the advantages of an LRAD-based volume monitor are its inexpensive simplicity, ruggedness, and its ability to detect contamination that is hidden from traditional alpha detection methods such as Geiger-Muller, gas cell, or solid-state detectors.

Traditional alpha detectors are designed to detect individual alpha particles and must not only be in direct line of site of the contamination, but also in the immediate area of the contamination. This is because alpha particles travel directly out from their source and have a very short range. Within just a few centimeters of their source, the alpha particles lose all of their energy to collisions with air particles, creating many ions. This makes it difficult or impossible to see contamination in small spaces such as cracks or on other surfaces inaccessible to the detector.

However, the ions created by the alphas can escape from small cracks or from behind enclosures and travel several meters. The LRAD is designed to collect these ions and therefore can detect contamination that is inaccessible to traditional alpha detectors. In addition, a single alpha particle creates 140,000 ion pairs, and so, even if only a fraction of these ions make it to the LRAD, they will produce a large signal. In contrast, a traditional alpha detector produces a signal only if struck by individual alpha particles. Adding high airflow to the LRAD technology greatly extends its capability.

APPLICATION

With the increase of nuclear waste, there is an increase in the need for its safe transport, storage, and disposal. In order to maintain a safe working environment for personnel and to comply with federal regulations, an accurate set of radiation monitoring tools is required. In addition, cost considerations demand devices which are simple to build and operate, reliable, and rugged enough to withstand potentially harsh environments. For example, a truck installed with a detector system for continuous monitoring must withstand and operate in environments with large temperature fluctuations and with high vibration and motion shock. A detector continuously monitoring an underground vault may have to endure very dusty or damp conditions.

The design of the HAFM is extremely rugged and simple to build, operate, and maintain. For these reasons, we believe the HAFM could be a valuable element in the monitoring and assay of nuclear waste transport, storage, and disposal. The HAFM is well suited for the monitoring of large volumes such as cargo vehicles, storage vaults, and rooms which may be exposed to radioactive waste. Surface contamination can result from storage containers that are poorly prepared or that have small leaks, which can be very small and difficult to reach with traditional alpha detectors. In addition, checking every square foot of container and vault surface can be impractical.

However, with the HAFM this kind of contamination can be assayed very easily. All surfaces can be monitored simultaneously because the fan on the stationary detector pulls ions into the detector

from throughout in the room. There is a limit to the detector sensitivity, however, dependent upon the size of the room and number of barriers between the contamination and the detector. As will be shown below, however, preliminary tests of the HAFM in a van indicate it has good sensitivity to alpha emitters.

For comparison, Table I shows potential applications for LRAD-based and traditional alpha detectors, including overlapping applications.

Table I. Comparison of HAFM and traditional alpha detector applications.

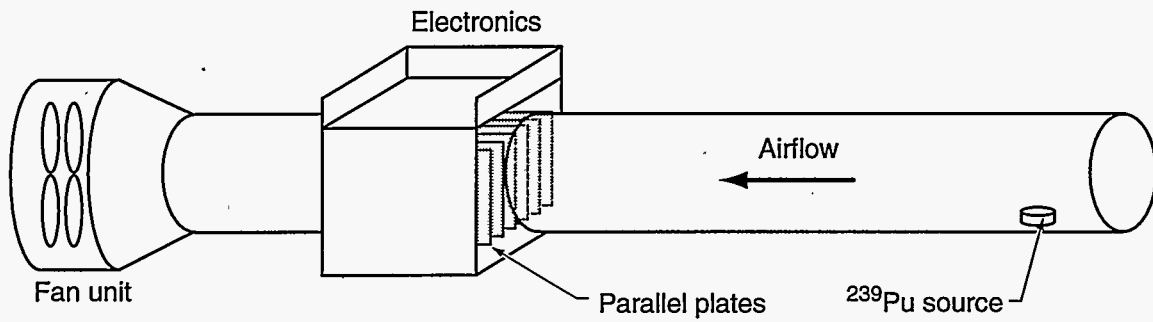
HAFM	HAFM and Traditional Alpha Detectors	Traditional Alpha Detectors
Survey multiple and/or large surfaces simultaneously	Close (5-cm), exposed surface contamination	Pinpoint location of contamination
Survey hidden and/or inaccessible surfaces	Real-time assay	Particle energy identification

HIGH AIRFLOW MONITOR OPERATION

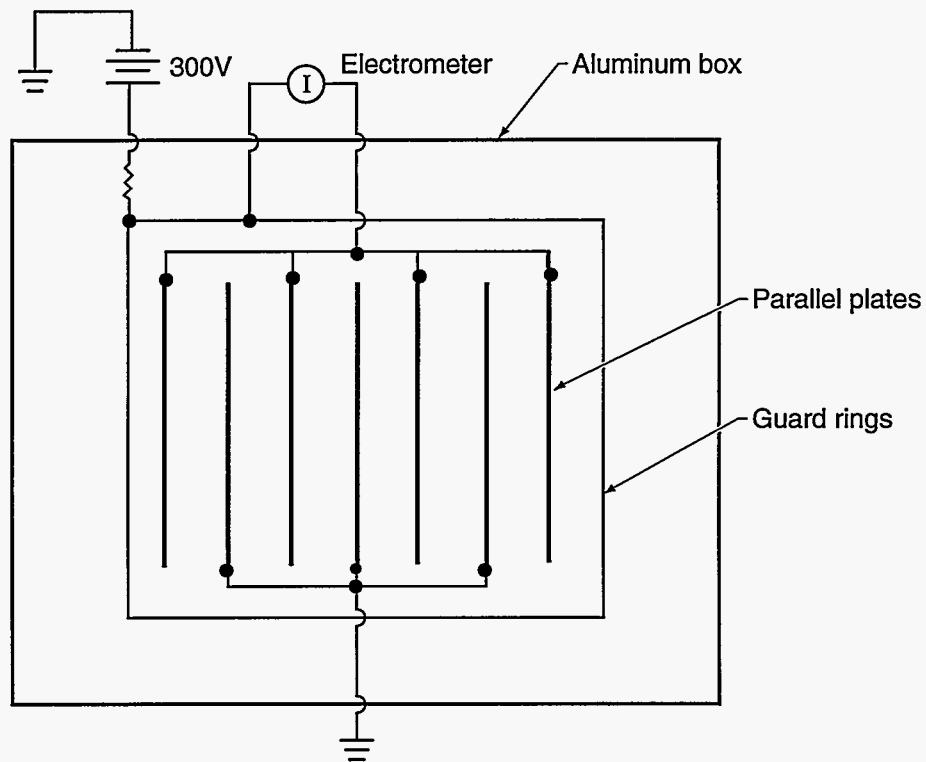
The high airflow LRAD design is shown in Fig. 1a. It consists of two to seven parallel plates aligned along the direction of airflow. A fan pulls air at high speed (50-400 cm/s) from the volume to be monitored, such as a room, storage vault, or cargo volume, into the detector. Voltage of up to 600 V is applied to alternate plates while the remaining plates are at ground potential. The ions of oxygen and nitrogen moving through the detector collect on the high-voltage (HV) plates and create a current proportional to the number of ions in the air. This current is extremely small (10^{-12} - 10^{-15} A) and has hampered the development of this technology until recently. Now, very sensitive electrometers are available to measure these small currents, and are small enough (wrist-watch size) to be carried on portable devices.

The high airflow through the detector enables more of the ions in the monitored volume to arrive at the detector before they recombine with other ions and become neutral again [2]. The finite lifetime of the ions is determined largely by their interaction with the surfaces and objects in the volume. Turbulent airflow can increase collisions with detector walls, reducing the signal, and is therefore undesirable. In low airflow LRAD designs, the plates are perpendicular to the airflow, and would introduce great turbulence and reduce the airflow rate if used in a high airflow application. The smooth airflow (more laminar) present using the parallel plate design reduces the turbulence, thus increasing detector sensitivity.

Since the detector monitors such small currents, effort must also be made to reduce false signals from currents leaking through insulators. These so called leakage currents can be comparable to and even larger than the signal from alpha emitters. Leakage currents can be reduced greatly by using a guard plate or ring between the signal plate and other paths to ground potential. The guard ring is at the same HV as the signal plates, and so the signal current will not take a path through the guard ring to ground. Figure 1b illustrates the electrical layout of the HAFM, including the guard ring. The resistor is in place mainly for electrical safety to reduce the current if someone contacts the HV plates.



(a)



(b)

Figure 1. Schematic diagrams of High Airflow Monitor. Figure 1a shows the mechanical layout and Fig. 1b shows the electrical layout.

Figure 2 shows a two-plate detector to illustrate the dependence of the detector signal on each of the parameters which characterize the detector. Here, L is the detector plate length, V_p is the plate voltage, S is the plate separation, and F is the airflow rate. The quantity c is a constant representing the drift rate or diffusion of ions in an electric field, and has units of $\frac{cm}{s} / \frac{V}{cm}$.

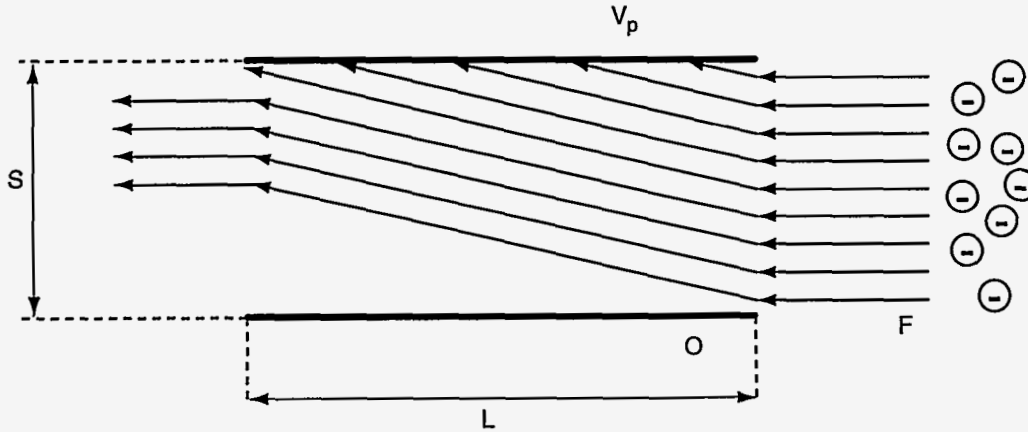


Figure 2. Diagram of High Airflow Monitor parameters for a two-plate configuration. S is the plate separation, V_p is the applied positive voltage, L is the plate length, and F is the airflow rate. Shown are the negative ions being attracted to the top plate at potential V_p . The bottom plate is at ground potential and attracts positive ions.

An incoming ion at the bottom plate will pass through the detector in a time L/F . In order to be detected, the ion must drift in the electric field up to the second plate in an equal or lesser time. The time for this drift is $\frac{S^2}{cV_p}$. Therefore, 100% efficiency ideally is given by

$$V_p = \frac{S^2 F}{cL} \equiv V_m \quad , \quad \text{Eq. (1)}$$

where V_m is the voltage at which the signal saturates. If $\frac{S^2}{cV_p}$ is twice as large as L/F , the efficiency is 50%. The efficiency can therefore be written

$$\epsilon_p = \frac{L}{F} \frac{S^2}{cV_p} = \frac{cV_p L}{S^2 F} \quad , \quad \text{Eq. (2)}$$

The ideal response of the detector is then

$$I = I_m \epsilon_p = \begin{cases} I_m \frac{cV_p L}{S^2 F} & V_p \leq V_m \\ I_m & V_p > V_m \end{cases} \quad , \quad \text{Eq. (3)}$$

which for $V_p \leq V_m$ is linear in the applied voltage V_p with slope

$$= I_m \frac{cL}{S^2 F} \quad , \quad \text{Eq. (4)}$$

Here, I is the detector current, and I_m is the saturation, or maximum, current.

Although the detector response does not follow Eq. (3) exactly, it is linear at low voltages and enables a determination of the diffusion constant c . These results are given in the data section below.

EXPERIMENTAL DATA

The HAFM shown in Fig. 1a is a seven-plate LRAD design. This represents one of several plate configurations tested for the combination of optimum detection efficiency and simplicity of construction. Several other parameters were also varied, including airflow rate, voltage applied to the

plates, plate separation, and collection of the signal from the plates at either HV or at ground potential.

The detector opening is a 9 cm inner diameter aluminum pipe, followed by a 15 cm x 15 cm x 16 cm aluminum box containing the parallel plates. This is followed by a 9-cm exit pipe and fan. The measurements were performed using a 192,000-disintegrations-per-second (192 kdps) ^{239}Pu source 65 cm from the front of the detector plates. Voltage to the plates was provided by combinations of batteries between 1.5 and 300 V, and the current was measured using an electrometer constructed in-house. The electrometer has a 0-1 V output for convenience, and this is the output signal used in plotting the results.

Source-In-Pipe Study

Figure 3 shows the data taken for several plate configurations ranging from two plates spaced 7.6 cm to seven plates spaced 1.3 cm. All error bars are smaller than the data symbols. Figure 3a shows the detector response at $F=400$ cm/s with the signal taken from the HV plates. Figure 3b shows the same for $F=50$ cm/s. For the 50 cm/s data, notice that the signal levels off at ~ 225 mV independent of the number of plates. This is the saturation signal, and indicates that essentially all of the ions making it to the detector are collected; i.e., none pass through the detector. The same is true for the 400 cm/s data, but the saturation signal is higher at 350 mV. The higher airflow results in a higher signal because a shorter transit time to the detector results in more ions making it to the detector. That is, because of the ion recombination half-life, a shorter transit time to the detector means more ions make it to the detector before they recombine. For example, in the case of ion transport in pipes, studies have found an ion half-life of 8.4 ± 2 s. [3]. The curves are fits to the data, and are described below.

Figures. 3c and 3d show data for an airflow of 400 cm/s and 50 cm/s with the signal taken from the plates at ground potential. The curves shown simply connect the data points. Again the 400 cm/s data produces the larger of the two signals. However, they are smaller than the corresponding signals from the HV plates. In addition, the signals fall off at high voltages. Both of these effects are due to fringe electric fields from the HV plates. The fringe fields create a collection plate for positive ions out of the pipe walls, and this competes with the ground collection plates for a signal. This effect is not present in the case of signal taken from the HV plates because there only the negative ions are collected.

For cases 3a and 3b, the signal is linear at low voltage and levels out at high voltage, as described by Eq. 3. However, the signal deviates from Eq. 3 at intermediate voltages. An attempt was made to find an equation which better describes the data of Figs. 3a and 3b. The desired equation should have a slope given by Eq. 4 at $V_p=0$ V, and approach zero slope at high voltage. The curves shown in Figs. 3a and 3b were obtained by fitting the data to

$$I = I_m \left(1 - e^{-\frac{V \ln 2}{V_c}} \right), \quad (5)$$

where V_c is the voltage which produces $I = 1/2 I_m$. At $V_p = 0$, Eq. 5 has a slope of

$$\text{slope} = \frac{I_m \ln 2}{V_c}, \quad (6)$$

which can be set equal to Eq. 4 to give

$$V_c = \frac{S^2 F \ln 2}{cL} \quad (7)$$

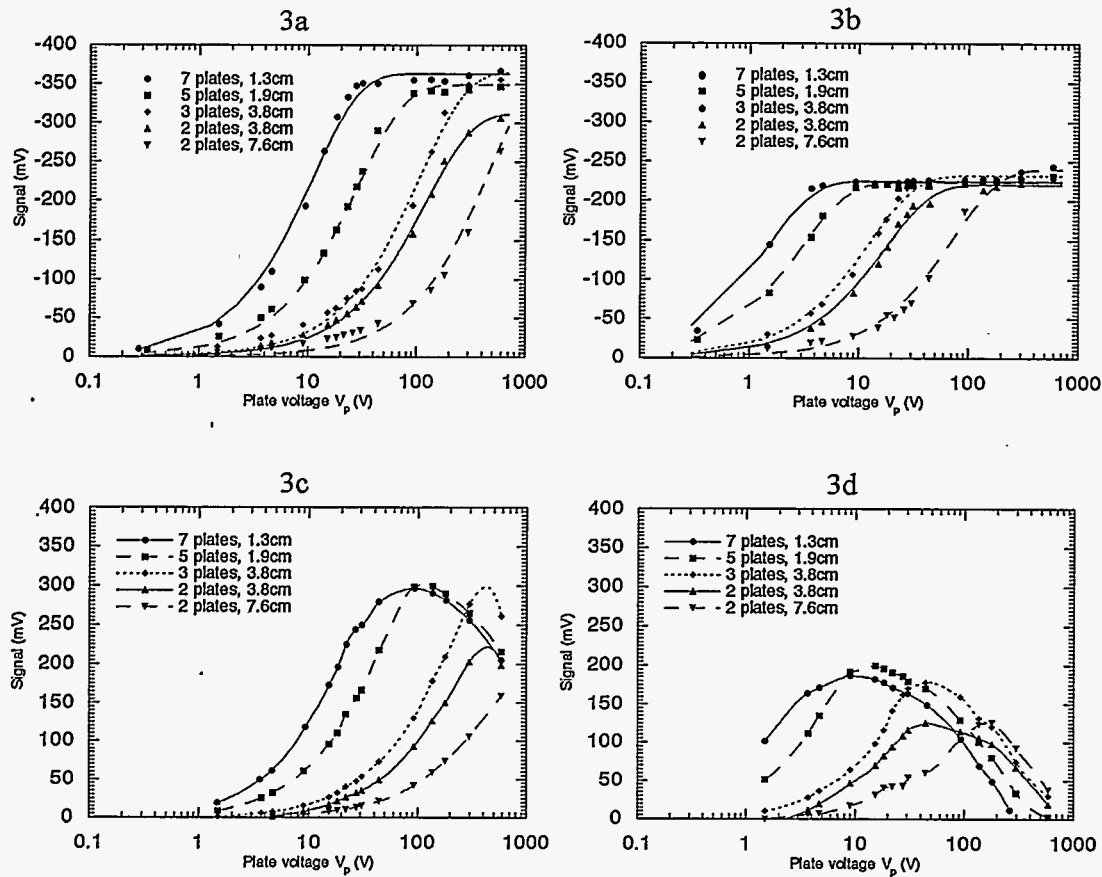


Figure 3. Response of the HAFM to various plate separations, airflow rates, and signal origins. Figure 3a shows the detector response for the signal taken from the high-voltage plates for an airflow of 400 cm/s. Figure 3b shows the same for an airflow of 50 cm/s. Figures 3c and 3d show the signal from the ground plates at 400 cm/s and 50 cm/s, respectively.

Eq. 7 can be solved for c to obtain experimental values of the diffusion constant. These results are shown in Table II, and are within a factor of 2 to 3 of much more precise measurements of ion mobility [4].

The value of V_c obtained from the fitted curves can also be compared to the functional dependence of Eq. 7. Table II shows experimentally determined values of V_c , V_c/F , and V_c/S^2 . The dependence on F is in good agreement with Eq. 7 as seen by the consistency of values in the rows of V_c/F . The dependence upon S^2 is not as good as for F , but the values of V_c/S^2 down the columns are also fairly consistent.

Table II. Experimentally determined values of c , V_c , V_c/F , and V_c/S^2 for plate geometry vs. airflow F . Least square fitting errors for c and V_c are in parentheses below the values.

F(cm/s) →	$c \left(\frac{cm}{s} / \frac{V}{cm} \right)$			$V_c(V)$			$V_c/F(Vs/cm)$			$V_c/S^2(V/cm^2)$		
	400	200	50	400	200	50	400	200	50	400	200	50
2 plates, 7.6 cm separation	6.6 (0.5)	5.2 (0.6)	2.7 (0.2)	336 (64)	185 (19)	49.9 (3.8)	42.0	46.2	49.9	37.3	20.5	5.5
2 plates, 3.8 cm separation	5.3 (0.1)	4.1 (0.1)	2.2 (0.1)	83.7 (2.8)	42.4 (1.5)	12.0 (0.5)	10.5	10.6	12.0	37.2	18.8	5.3
3 plates, 3.8 cm separation	5.3 (0.2)	5.1 (0.1)	2.8 (0.1)	74.2 (4.2)	35.5 (2.1)	8.7 (0.3)	9.3	8.9	8.7	33.0	15.8	3.9
5 plates, 1.9 cm separation	3.7 (0.2)	3.1 (0.3)	2.3 (0.3)	20.2 (0.4)	9.7 (0.4)	2.1 (0.1)	2.5	2.4	2.1	35.9	17.2	3.7
7 plates, 1.3 cm separation	2.9 (0.1)	2.7 (0.1)	1.3 (0.4)	7.6 (0.4)	4.0 (0.2)	1.0 (0.1)	0.95	1.0	1.0	30.4	16.0	4.0

Van Study

The above analysis shows the results of a very controlled geometry. The detector must also be tested in more realistic situations before its value as a vehicle or facility monitor can be established. Some preliminary data has been obtained for the detection of contamination in a van using the HAFM. The source of ions in these tests was several commercially available static control strips. These "Static Master" devices are composed of alpha-emitting ^{210}Po with a half life of 138 days, nominally 500 mCi when manufactured.

The van study included data measurements for the source at different locations, measurements after the source was in the van for several minutes and immediately following addition of the source, and different airflow rates. In addition, the effect of opening a door, and the effect of the van being in direct sunlight or not, was monitored. Figure 4 shows the detector response in these situations. The signal varies for these different tests, but the signal was always clearly visible above the background, indicating the HAFM is a viable technique for monitoring large volumes.

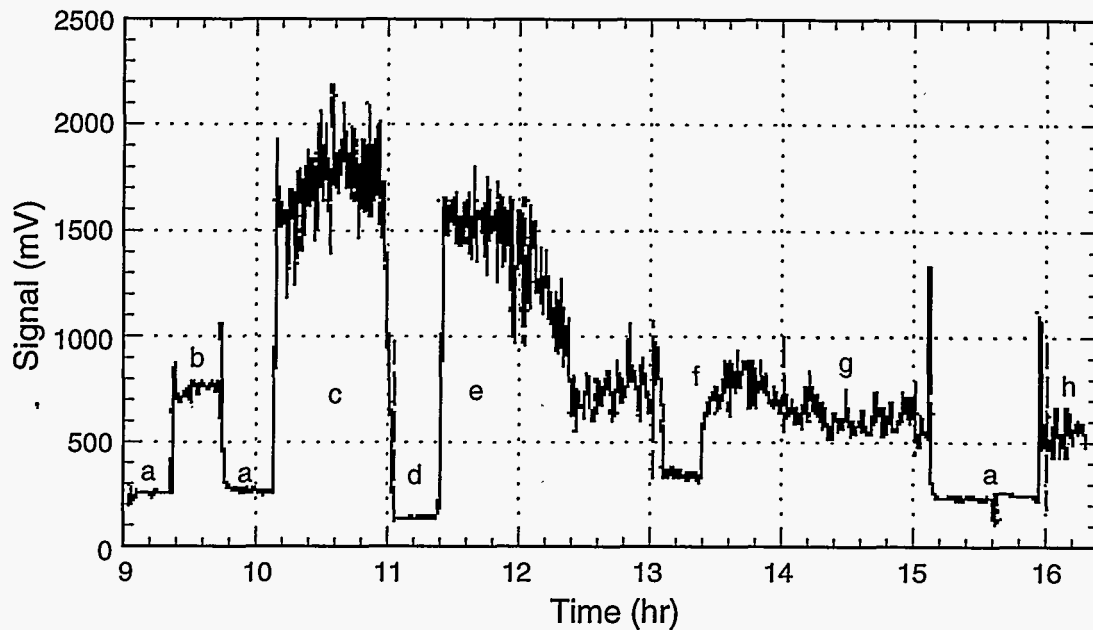


Figure 4. Realtime response of the HAFM placed within a passenger van with different airspeeds and radioactive source locations. The following regions are evident: (a) Background signal inside van. (b) source location is second row of seats. (c) Source location is third row of seats. (d) Background outside of van. (e) Source located on third row seats for several minutes before signal taken; also effect of van entering shadow of sunlight (f, g) Signal for several airflow rates with source on third rows of seats. (h) Source location is fourth row of seats.

SIMULATION WORK

In an effort to refine the HAFM, we are beginning a study to simulate the airflow characteristics of rooms and vehicles. This effort will identify general requirements for detector size, placement, and airflow rate for maximum detector sensitivity. There are several codes available which do computational fluid dynamics and/or ion interaction, and others that can numerically map the geometry of rooms and objects within them. However, a code which integrates all of these, as required by the current problem, is not available.

The current effort in this area involves (a) determining which codes to use and integrating their input and output requirements and (b) constructing an HAFM which has an axially symmetric source of ions and which produces an axially symmetric and laminar airflow. Data from the latter is necessary for comparison to initial calculations because of the large computation times required for true three-dimensional simulations. An axially symmetric detector has been constructed and is currently under test.

Simulations of this type have been used successfully in other applications. A code developed by the US Army High Performance Computing Research Center at the University of Minnesota, and under consideration for this work, was used successfully to simulate the dispersion of a chemical contaminant through the Tokyo subway. The present application concerns a much smaller geometry but is complicated by the need to draw conclusions about volumes of arbitrary size and contents and the need to describe not only flow patterns of the ions but also the recombination of ions within the volume and at the walls.

CONCLUSIONS

The LRAD-technology-based High Air Flow Monitor has been examined for sensitivity as a function of number of plates, plate voltage, plate separation, airflow rate, and electrical potential of the signal-source plate. The results indicate a preference for a collection voltage of 300 V, the use of at least five plates, and an airflow of at least 400 cm/s. In addition, the signal should be taken from the plates at high voltage to avoid competing with the pipe walls for signal due to fringe fields.

The HAFM shows promise as a detector for the assay of radioactive waste transport vehicles, storage vaults, and other moderately sized rooms. Multiple HAFMs could be incorporated to monitor even larger rooms. The proof of principle has been shown for the case of a source placed within a van, which has complicated internal surfaces.

Work to simulate the airflow and ion recombination in rooms is underway. Data from an axially symmetric detector will be compared to calculations in simple shaped rooms initially, followed by calculations for more complicated volumes. These calculations may reveal a problem with detector size, placement within a volume, or airflow rate which has eluded current experimental tests. The calculations may also provide answers to questions more quickly than is possible by detector redesign and testing. The conclusions from these simulations will then be used to optimize the HAFM for vehicle and room size volumes.

REFERENCES

1. D. W. MacArthur et al., *Long-Range Alpha Detector*, Health Physics 63: 324-330, (September, 1992).
2. J. E. Koster et al., *Real-Time Monitoring for Alpha Emitters in High-Airflow Environments*, Proceedings, Nuclear and Hazardous Waste Management International Topical Meeting (SPECTRUM '96) (August, 1996).
3. S. P. Rojas et al., *Alpha Characterization Inside Pipes Using Ion-Transport Technology*, Proceedings, Waste Management '95, Folio Infobase CD-ROM, (March, 1995).
4. V.A. Mohnen, *Formation, Nature, and Mobility of Ions of Atmospheric Importance*, in Electrical Processes in Atmospheres, Hans Dolezalek and Reinhold Reiter eds., Verlag, Darmstadt, Germany (1977).